JOURNAL OF GUIDANCE, CONTROL, AND DYNAMICS
Vol. 17, No. 5, September–October 1994

# New Technique for Nonlinear Control of Aircraft

M. Asif Khan* and Ping Lu†
*Iowa State University, Ames, Iowa 50011*

**A newly developed methodology for design of nonlinear feedback controllers is applied to aircraft control. Using a high-performance aircraft model, we evaluate the controller performance under a variety of strenuous conditions. The controller performance is further enhanced by optimally adjusting a controller parameter continuously and incorporating derivative feedback. The robustness of the controller is demonstrated by achieving satisfactory performance in the presence of large system uncertainties and external disturbances. Finally, novel applications of this control technique in point-to-point control of aircraft are presented.**

## Nomenclature

| | |
|---|---|
| $D$ | = drag force, lb |
| $d$ | = down-range distance, ft |
| $g$ | = gravitational acceleration, ft/s$^2$ |
| $h$ | = altitude, ft |
| $I_y$ | = moment of inertia, slug-ft$^2$ |
| $L$ | = lift force, lb |
| $m$ | = total aircraft mass, slug |
| $q$ | = pitch rate, deg/s |
| $T$ | = total thrust for two engines, lb |
| $t$ | = time, s |
| $U$ | = control set |
| $V$ | = velocity, ft/s |
| $W_x$ | = horizontal wind speed, ft/s |
| $\alpha$ | = angle of attack, deg |
| $\delta_H$ | = symmetric stabilator deflection, deg |
| $\delta_T$ | = throttle setting, deg |
| $\theta$ | = pitch angle, deg |
| $\Sigma M$ | = total body axis pitching moment, ft-lb |

## I. Introduction

TODAY'S high-performance aircraft often operates in regimes where angle of attack is high and angular rates are large. In other cases the trajectory of the aircraft may cover a large flight envelope. In these situations, nonlinearities become a predominant feature of the aircraft dynamics. The flight control system needs to respond to these nonlinearities to achieve satisfactory performance. A popular approach for nonlinear flight control law design is dynamic inversion. In this approach, the nonlinearities are canceled by static feedback and the dynamics are replaced by desired linear dynamics. Successful applications have been demonstrated in the literature (e.g., Refs. 1–5). Actual implementation of this technique in flight control systems has also been reported.[6] This paper proposes a new approach for nonlinear flight controller design. The approach is based on a methodology recently developed by Lu[7] for nonlinear control law synthesis. The control law is constructed based on minimization of local errors between the controlled variables and their desired values. This approach is systematic, requires no stringent conditions on the system other than the usual smoothness conditions, and is often effective. In this paper, this technique is applied to a realistic high-performance aircraft model. Further improvements are made to enhance the performance of the controller. The applications encompass aspects of control of the aircraft through large portion of the flight envelope, robustness in the presence of disturbances and system uncertainties, and point-to-point control of the aircraft. The rest of the paper is organized as follows: Section II briefly describes the method used to derive the baseline controller. The model for a realistic advanced fighter aircraft is introduced and the control objective is explained in Sec. III. In Sec. IV, the performance of the baseline controller is demonstrated. Then modifications are made to the baseline controller to further enhance its performance. Section V evaluates the robustness of the controller in the presence of modeling uncertainties and wind disturbance. In Sec. VI, applications of the controller in point-to-point control of aircraft are discussed. Section VII summarizes the work.

Received Jan. 15, 1993; revision received Sept. 12, 1993; accepted for publication Nov. 13, 1993. 

*Graduate Student, Department of Aerospace Engineering and Engineering Mechanics. Student Member AIAA.

†Assistant Professor, Department of Aerospace Engineering and Engineering Mechanics. Senior Member AIAA.

## II. Baseline Controller Development

For the convenience of reference, the derivation of the basic controllers[7] is briefly reviewed in this section. Suppose that the dynamic equations for a nonlinear control system have the form

$$\dot{x}_1 = f_1(x) \tag{1}$$

$$\dot{x}_2 = f_2(x) + B(x)u \tag{2}$$

where $x_1 \in \boldsymbol{R}^{n_1}$, $x_2 \in \boldsymbol{R}^{n_2}$, and $n_1 + n_2 = n$. Here $x^T = (x_1^T\ x_2^T) \in \boldsymbol{R}^n$ is the state of the system. $u \in \boldsymbol{U} \subset \boldsymbol{R}^m$ is the control vector, and $\boldsymbol{U}$ is a compact set that defines the feasible controls. The function $f_1$ is sufficiently differentiable, and $f_2$ and $B$ need only to be $C^1$. Equations (1) usually represent the kinematics in the system and Eqs. (2) the dynamics. Suppose that a reference trajectory $s(t) \in R^n$, $t \in [t_0, t_f]$, is given. It is assumed that $s(t)$ satisfies the state equations (1) and (2) with some reference control $u^*(t) \in \boldsymbol{U}$, although $u^*(t)$ need not be known explicitly. The trajectory $s(t)$ can be obtained off-line through an optimization process or may be defined onboard, as will be discussed in Sec. VI. We assume here that $s(t)$ represents the desired state history, but it can also be desired output history. Partition $s(t)$ into $n_1$- and $n_2$-dimensional vectors

$$s(t) = \begin{pmatrix} s_1(t) \\ s_2(t) \end{pmatrix} \tag{3}$$

For simplicity of presentation, we will assume that the second-order derivative of each component of $x_1$ contains components of the control $u$ explicitly, since this is the case for our application in this paper. Suppose that at an arbitrary $t_k \in [t_0, t_f)$, the state $x(t_k)$ is known. Consider $x(t_{k+1}) = x(t_k + \Delta)$, where $\Delta > 0$ is the time increment. Expanding $x_1(t_{k+1})$ in a second-order Taylor series expansion and $x_2(t_{k+1})$ in a first-order expansion, we have

$$\begin{aligned} x_{1_{k+1}} \approx\ & x_{1_k} + \Delta f_1(x_k) + \tfrac{\Delta^2}{2}[F_{11} f_1(x_k) + F_{12} f_2(x_k) \\ & + F_{12} B(x_k) u_k] x_5 \end{aligned} \tag{4}$$

$$x_{2_{k+1}} \approx x_{2_k} + \Delta[f_2(x_k) + B(x_k)u_k] \tag{5}$$

where $F_{11} = \partial f_1(x_k)/\partial x_1$ and $F_{12} = \partial f_1(x_k)/\partial x_2$. The state tracking errors at time $t_k + \Delta$ are $e_{1_{k+1}} = x_{1_{k+1}} - s_{1_{k+1}}$ and $e_{2_{k+1}} = x_{2_{k+1}} - s_{2_{k+1}}$. The minimization of the performance index

$$J_k = \tfrac{1}{2} e_{1_{k+1}}^T Q_1 e_{1_{k+1}} + \tfrac{1}{2} e_{2_{k+1}}^T \Delta^2 Q_2 e_{2_{k+1}} \tag{6}$$

minimizes the weighted tracking errors, where $Q_1$ and $Q_2$ are positive semidefinite square matrices of the appropriate dimensions. This performance index is quadratic in $u_k$ when $x_{1_{k+1}}$ and $x_{2_{k+1}}$ are approximated by Eqs. (4) and (5). Expanding the reference trajectory $s_{1_{k+1}}$ and $s_{2_{k+1}}$ in similar ways gives

$$s_{1_{k+1}} \approx s_{1_k} + \Delta \dot{s}_{1_k} + \tfrac{1}{2}\Delta^2 \ddot{s}_{1_k} \tag{7}$$

$$s_{2_{k+1}} \approx s_{2_k} + \Delta \dot{s}_{2_k} \tag{8}$$

Then $J_k$ has a unique minimum at $\partial J_k/\partial u_k = 0$. Solving for the $u_k$ that satisfies this expression yields

$$u(t_k) = -W_k^{-1}\left(\frac{1}{2\Delta^2} G_k^T Q_1 P_{1k} + \frac{1}{\Delta} B^T(x_k) Q_2 P_{2k}\right) \tag{9}$$

where the following substitutions have been made:

$$G_k = F_{12} B(x_k) \tag{10}$$

$$W_k = \tfrac{1}{4} G_k^T Q_1 G_k + B^T(x_k) Q_2 B(x_k) \tag{11}$$

$$P_{1k} = e_{1_k} + \Delta \dot{e}_{1_k} + \tfrac{1}{2}\Delta^2 (F_{11} f_1(x_k) + F_{12} f_2(x_k) - \ddot{s}_{1_k}) \tag{12}$$

$$P_{2k} = e_{2_k} + \Delta (f_2(x_k) - \dot{s}_{2_k}) \tag{13}$$

Since the time $t_k$ is arbitrarily chosen as any point in the interval $[t_0, t_f)$, we have a continuous, nonlinear feedback control law

$$u(t) = -W^{-1}\left(\frac{1}{2\Delta^2} G^T Q_1 P_1 + \frac{1}{\Delta} B^T(x) Q_2 P_2\right) \tag{14}$$

For more complete and rigorous derivations and discussions, we refer the reader to Ref. 7. This controller has various desirable properties. It involves only the Jacobians of $f_1(x)$. Typically $f_1(x)$ specifies the kinematic relations of the system and thus is analytically defined. This results in $F_{11}$ and $F_{12}$ being simple to obtain. The parameter $\Delta$ need not be the "integration step size." It can be treated as a controller parameter that can be adjusted to improve the performance of the controller. If the errors are zero at one point, it can be shown that the reference trajectory is exactly tracked afterward (i.e., if $e(t_1) = 0$, then $e(t) \equiv 0$ for all $t \in [t_1, t_f]$). Note that the number of the controlled variables need not be equal to that of the controls. If this is true, however, the controller works in a similar way as dynamic inversion does with the desired linear dynamics having a damping ratio of 0.707. Consequently, asymptotic tracking is guaranteed, provided no control saturation occurs. When the control computed from Eq. (14) exceeds the control bounds, the use of the maximum (or minimum) allowable control has a clear physical meaning: It is still the best choice within the control bounds that minimizes the performance index (6). In contrast, the dynamic inversion approach encounters difficulty in determining the control strategy in the presence of control saturation, since feedback linearization is not achievable in such a case. It can also be established that the controller is robust in the presence of a class of modeling uncertainties. This baseline controller is referred to as controller I.

## III. Aircraft Model and Reference Trajectory

To demonstrate the practical applicability of this control technique, a complex realistic aircraft model is used in this study. The aircraft model was based on the model for the 1991–1992 AIAA Controls Design Challenge.[8] Some minor modifications have been made.[9] The model is a generic, state-of-the-art, high-performance aircraft. It has nonlinear aerodynamics, defined over the entire operational flight envelope of the aircraft. The aerodynamic coefficients and thrust level are computed by performing multidimensional, linear interpolations of tabular data. This results in an aircraft model that is representative of a "real" aircraft for which experimental data are typically available. The aircraft weighs 45,000 lb and has a wing area of 608 ft$^2$. It is approximately the same size as the F-15 Eagle. The primary control surfaces of the aircraft are two stabilators, two ailerons, and a rudder on a single vertical tail. The aircraft has two turbofan engines capable of producing 34,000 lb of thrust each and has a maximum speed of Mach 2.5. The absolute ceiling of the aircraft is approximately 60,000 ft. The original aircraft model has six degrees of freedom. In this study, the application is limited to two-dimensional flight in the vertical plane for simplicity. It should be noted that this is not necessary in view of the generality of the controller design methodology. The aircraft dynamics for vertical planar flight are defined by the following equations of motion[9]:

$$\dot{V} = \frac{1}{m}[-D + T\cos\alpha - mg(\sin\theta\cos\alpha - \cos\theta\sin\alpha)] \tag{15}$$

$$\dot{\alpha} = \frac{1}{Vm}[-L - T\sin\alpha + mg(\cos\theta\cos\alpha + \sin\theta\sin\alpha)] + q \tag{16}$$

$$\dot{\theta} = q \tag{17}$$

$$\dot{q} = \Sigma M / I_y \tag{18}$$

$$\dot{h} = V(\cos\alpha\sin\theta - \sin\alpha\cos\theta) \tag{19}$$

$$\dot{d} = V(\cos\alpha\cos\theta + \sin\alpha\sin\theta) \tag{20}$$

The state variables needed in the control laws are assumed to be either measured or estimated. The reference trajectory is a minimum time-to-climb trajectory. A detailed description of the method used to obtain the trajectory is in Ref. 10. The trajectory leads from takeoff at sea level to a final altitude of 50,000 ft in the shortest time possible. The initial conditions for this reference flight path are

$$v_0 = 400 \text{ ft/s}, \qquad \alpha_0 = \theta_0 = 5 \text{ deg}, \qquad q_0 = h_0 = d_0 = 0 \tag{21}$$

Designing control laws to follow this flight path is a very challenging task. The Jacobian matrix of the system is discontinuous because of the linear interpolations used for aerodynamic and propulsion modeling. Therefore, the standard linearization is only valid, if valid at all, in a very small neighborhood of the reference point. Yet the range of variations of the state variables along the desired trajectory is very large. Along the reference trajectory, the aircraft is operating at a throttle (power lever angle) setting close to the maximum value (127 deg out of the range between 20 deg and 135 deg). In addition, a large portion of the trajectory is flown at low Mach numbers and high altitudes. In such flight conditions, the effectiveness of the control surfaces is considerably reduced. These factors dictate that control saturations can easily occur, indicating that dynamic inversion may not be a suitable control approach either.

## IV. Flight Control Laws

### A. Controller I: Baseline Controller

To apply controller I [Eq. (14)], we partition the aircraft state vector in the form described by Eqs. (1) and (2),

$$x_1 = \begin{pmatrix} \theta \\ h \\ d \end{pmatrix}, \qquad x_2 = \begin{pmatrix} V \\ \alpha \\ q \end{pmatrix}, \qquad u = \begin{pmatrix} \delta_H \\ \delta_T \end{pmatrix} \tag{22}$$

where the two control inputs are the symmetric stabilator deflection $\delta_H$ and the throttle setting $\delta_T$. The dynamic equations are Eqs. (15), (16), and (18); kinematic equations are Eqs. (17), (19), and (20). The control limits are enforced by simple limiters. The control law in Eq. (14) is used when no saturations occur; the corresponding limit value is used if any of the controls saturate. For testing this baseline controller, off-nominal conditions are created by introducing perturbations to the initial conditions of the state variables. (If there were no initial perturbations, the nominal trajectory would be tracked exactly.) The performance of the controller is judged on how well the altitude history is followed. Two criteria are used. The maximum error $E_{\max}$ is the greatest difference between the nominal

**Table 1 Results for controllers I and II**

| Perturbation | Controller I | | Controller II | |
|---|---|---|---|---|
| | $E_{max}$, ft | $\bar{E}$, ft | $E_{max}$, ft | $\bar{E}$, ft |
| +80 ft/s, $v_0$ | 1110 | 239 | 9.1 | 0.4 |
| −80 ft/s, $v_0$ | 1570 | 821 | 1570 | 793 |
| +5 deg, $\alpha_0$ | 43.9 | 6.7 | | |
| −5 deg, $\alpha_0$ | 2000 | 1070 | 543 | 182 |
| +5 deg, $\theta_0$ | 2330 | 1290 | 1270 | 572 |
| −5 deg, $\theta_0$ | 80.9 | 14.4 | | |
| +8 deg/s, $q_0$ | 18.6 | 2.0 | | |
| −8 deg/s, $q_0$ | 10.0 | 1.2 | | |
| +200 ft, $h_0$ | 3640 | 2160 | 1220 | 544 |

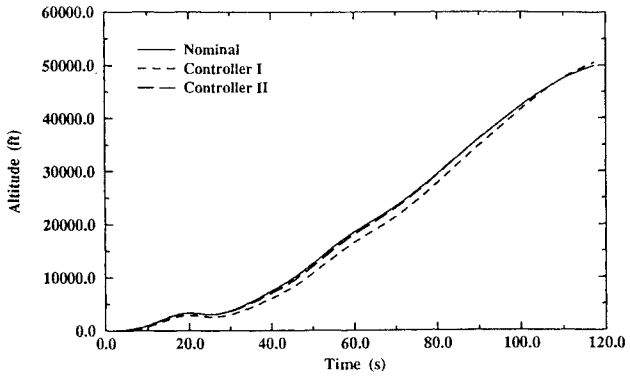


**Fig. 1 Controllers I and II: altitude history with −5 deg angle-of-attack perturbation.**

and actual altitude histories at any given time. The mean error $\bar{E}$ is defined by

$$\bar{E} = \frac{1}{t_f} \int_{t_0}^{t_f} |h_{\text{actual}} - h_{\text{ref}}| \, dt \tag{23}$$

The testing found that controlling two or three variables ensures a good tracking of the reference trajectory because of the coupling among the state variables. Altitude, of course, must be controlled. Of the remaining controlled variables, at least one must be an angle or angular rate to maintain stability of the aircraft. According to Eq. (6), a state variable will be controlled to follow its desired value if the corresponding element on the main diagonal of the weighting matrix $Q_1$ (or $Q_2$) is nonzero (positive). Otherwise, the error in this variable will not influence the controls. Our experience shows that the performance of the controller is extremely insensitive to the choices of the values of the weightings. On the other hand, the parameter $\Delta$ affects the performance of the controller to a great extent. For controller I, $\Delta$ was chosen to be a constant of 0.1 s.

The results for a number of initial perturbations are given in Table 1. Altitude and pitch angle were the two controlled variables. The actual initial conditions are the nominal values plus the values in the first column of Table 1. For some quite appreciable perturbations, the aircraft was able to follow the reference path very closely. The altitude and control histories of the case of −5 deg angle-of-attack perturbation are shown in Figs. 1 and 2. This is one of the least accurately followed cases among all cases tested. The results in Table 1 show that the controller provides good tracking of the nominal trajectory in majority of the cases, with two or three exceptions. The largest altitude error is less than 7.5% of the total height climbed. This is a noteworthy achievement considering that the perturbations in several cases are 100% of the initial state values. Figures 2 and 3 demonstrate the feedback nature of the controller. At the instant the aircraft "overshoots" the nominal trajectory, the throttle setting attempts to reduce the aircraft velocity by switching from the upper to the lower limit. Immediately after the 20-s mark, the throttle setting also switches to the lower limit for a brief period of time. This allows the aircraft to rapidly pitch up to a required attitude. For most test cases, though, the saturation of the throttle setting leads to a steady altitude error. Similar trends were observed when altitude and angle of attack were used as the controlled variables.

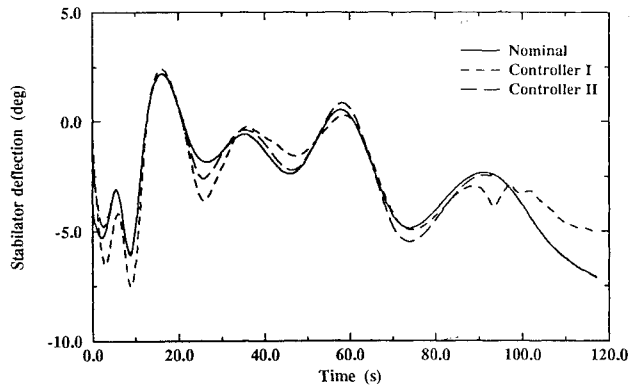


**Fig. 2 Controllers I and II: stabilator deflection history with −5 deg angle-of-attack perturbation.**

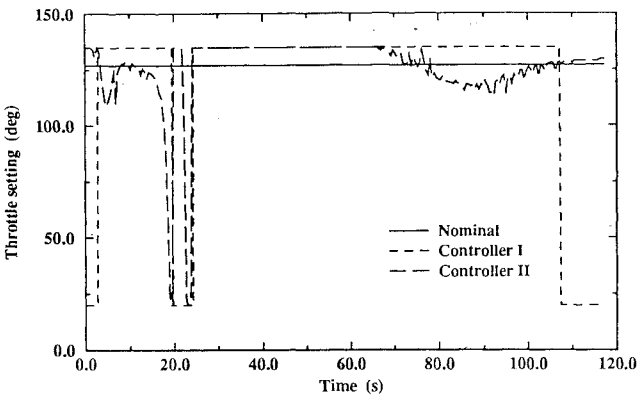


**Fig. 3 Controllers I and II: throttle setting history with −5 deg angle-of-attack perturbation.**

### B. Controller II: Optimal Tuning

During the preceding testing it was observed that the choice of the $\Delta$ parameter greatly affected the performance of the controller. For controller I, $\Delta$ is taken to be a constant throughout the time of flight of the trajectory. But from the control law development in Sec. II we realize that $\Delta$ is not necessarily a constant. In this section the controller is modified to allow a time-varying $\Delta$. From the discussion in Sec. II, we see that $J_k$ in Eq. (6) is a function of $\Delta$ with $x_{1_{k+1}}$ and $x_{2_{k+1}}$ approximated by Eqs. (4) and (5) and $u_k$ specified by Eq. (9). In this section, the $\Delta$ parameter is optimally chosen within a bounded range of [0.1, 30] to minimize the performance index $J_k$ at each instant when the controls are calculated. The one-dimensional minimization is performed by using Brent's algorithm.[11] This modified controller is called controller II.

Some of the "worst" cases from the controller I testing are repeated here. The results are also given in Table 1. In all the cases tested, controller II shows improvements over controller I that are quite noticeable in most cases. For instance, the altitude history of the case of −5 deg angle-of-attack perturbation is shown in Fig. 1. The enhancement in the tracking performance is very evident when compared to the trajectory under controller I in the same figure. The control histories are in Figs. 2 and 3. Figure 4 shows the variation of the optimal $\Delta$. From control law equation (14), it can be seen that $1/\Delta$ reflects the controller gain. Small $\Delta$ means high controller gain. Figure 4 indicates that the best gain is not necessarily always the highest ($\Delta = 0.1$). Instead, some modest gains were found to be optimal for most of the flight.

The optimization of the parameter $\Delta$ is fairly simple and can be performed online. Because of the nature of this one-dimensional optimization, the resulting controls may be discontinuous due to the discontinuities in computing the optimal $\Delta$. If the discontinuities are undesirable, a filter can be used to smooth the values of $\Delta$. Our tests showed that the small time lag caused by the filter has negligible effects on the overall performance.

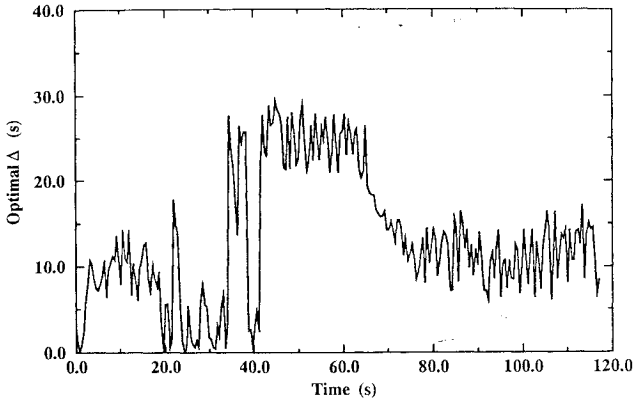


**Fig. 4 Controller II: optimal Δ history with −5 deg angle-of-attack perturbation.**

### C. Controller III: Derivative Feedback

We note that in the derivation of the basic controller, the performance index equation (6) that penalizes tracking errors is minimized. When the error $e_1$ is the primary concern, as in this application, an additional term involving $\dot{e}_1$ may be added to the performance index. This modification is expected to provide the controller with some anticipatory characteristics, similar to a proportional-plus-derivative controller in classical control theory. Thus the performance of the controller can be further improved. To this end, we consider the following performance index:

$$J_k = \tfrac{1}{2}e_{1_{k+1}}^T Q_1 e_{1_{k+1}} + \tfrac{1}{2}\dot{e}_{1_{k+1}}^T Q_2 \dot{e}_{1_{k+1}} + \tfrac{1}{2}e_{2_{k+1}}^T Q_3 e_{2_{k+1}} \tag{24}$$

where the $Q_i$ are positive semidefinite matrices. Note that $\dot{e}_1$ contains only velocities and angular rates, not accelerations, which are known to be very noisy. Repeating the procedure used to derive controller I, we obtain the following control law:

$$u(t) = -W^{-1}\left[\tfrac{1}{2}\Delta^2 G^T Q_1 P_1 + \Delta G^T Q_2 P_2 + \Delta B^T(x) Q_3 P_3\right] \tag{25}$$

where the following substitutions have been made:

$$G = F_{12}B(x) \tag{26}$$

$$W = G^T\left(\tfrac{1}{4}\Delta^4 Q_1 + \Delta^2 Q_2\right)G + \Delta^2 B^T(x) Q_3 B(x) \tag{27}$$

$$P = F_{11}f_1(x) + F_{12}f_2(x) - \ddot{s}_1 \tag{28}$$

$$P_1 = e_1 + \Delta\dot{e}_1 + \tfrac{1}{2}\Delta^2 P \tag{29}$$

$$P_2 = \dot{e}_1 + \Delta P \tag{30}$$

$$P_3 = e_2 + \Delta(f_2(x) - \dot{s}_2) \tag{31}$$

This control law is denoted as controller III. The test results for some perturbations in the initial conditions are given in Table 2. The results show significant reductions in the maximum and mean errors compared to the results of controller I. In some cases the errors have been reduced by as much as 90%. From Tables 1 and 2, we see that in general controller III also offers better performance than controller II. In the case of −5 deg angle-of-attack perturbation, the values of $\bar{E}$ are about the same but controller III reduces $E_{\max}$ significantly. This is typical of a derivative feedback controller. The value of Δ used in the tests was 1.0 s. Optimization of Δ in controller III is not expected to further reduce the errors in this application, since the remaining errors are mostly due to throttle-setting saturation. To test the capability of controller III, we even used some unrealistically large initial perturbations (e.g., a −20 deg perturbation in $\alpha_0$ and +50 deg in $\theta_0$). In these extreme cases, the largest deviation is only 2.0% of the final altitude.

**Table 2 Controller III results**

| Perturbation | $E_{\max}$, ft | $\bar{E}$, ft |
|---|---|---|
| +80 ft/s velocity | 7.4 | 4.9 |
| −80 ft/s velocity | 480 | 429 |
| −5 deg angle of attack | 183 | 167 |
| −20 deg angle of attack | 547 | 460 |
| +5 deg pitch angle | 211 | 191 |
| +50 deg pitch angle | 628 | 520 |
| +200 ft altitude | 399 | 147 |
| +1000 ft altitude | 1000 | 206 |

## V. Controller Robustness

### A. External Disturbances

In the presence of system uncertainties and disturbances, it is desired that the controller maintain satisfactory performance. Our controllers are derived based on continuous minimization of the differences between the controlled variables and their desired values. This mechanization provides a certain degree of robustness. Some analytical robustness properties of the controller have been established by Lu.[7] To evaluate the robustness in this application, we first tested the controller in the presence of a horizontal wind. The wind velocity is modeled as a function of altitude,

$$W_x = \begin{cases} 80\cos(h\pi/10000) & \text{if } 0 \le h \le 25{,}000 \text{ ft} \\ 0 & \text{otherwise} \end{cases} \tag{32}$$

The dynamics of the aircraft including wind effects are[12]

$$\dot{V} = [T\cos\alpha - D - mg\sin(\theta - \alpha)]/m - \dot{W}_x\cos(\theta - \alpha) \tag{33}$$

$$\dot{\alpha} = [-T\sin\alpha - L + mg\cos(\theta - \alpha)]/mV - \dot{W}_x\sin(\theta - \alpha)/V + q \tag{34}$$

$$\dot{d} = V\cos\alpha + W_x \tag{35}$$

where

$$\dot{W}_x = \frac{\partial W_x}{\partial h}\dot{h} \tag{36}$$

Note that $V$ is the speed of the aircraft relative to the air, not inertial speed. The wind model represents a strong wind of 80 ft/s (55 mph) that starts with a tail wind on the ground, which affects takeoff adversely. The initial velocity of the aircraft relative to the air is then the nominal inertial velocity (400 ft/s) minus the 80 ft/s tail wind. The reference trajectory is still the same one used in the preceding sections. The test was conducted using controller III. The controller, which is based on the nominal (nowind) model, is given no information regarding the wind. All the terms involving the wind in Eqs. (33–35) are treated as unknown external disturbances, but the controller uses the true values of the state variables (assumed to be measured) from Eqs. (33–35) as feedback. The resulting trajectory is displayed in Fig. 5. The actual trajectory has a maximum error of 857 ft and a mean error of 403 ft. This is a very exceptional performance, given the magnitude of the wind. Note that in the same figure the aircraft trajectory flown with the open-loop optimal controls obtained in Ref. 10 crashed shortly after takeoff.

### B. System Uncertainties

To evaluate the performance of the controller in the face of system uncertainties, the controller was tested with errors added in the aerodynamic coefficients. The exercise was performed assuming that a ±30% error exists in all the stored aerodynamic data. The error was taken to simultaneously occur in the coefficients of lift, drag, and pitching moment, respectively. The testing was executed using controller III. The case of +30% errors has a maximum error of 628 ft and a mean error of 346 ft. The case of −30% errors is the worst one and has a larger maximum error of 1170 ft and a mean error of 436 ft. The altitude histories for the case of −30% errors are shown in Fig. 6. Again, with the nominal open-loop control, the aircraft crashed shortly after takeoff. These results show the impressive ability of the controller to control the aircraft in the presence

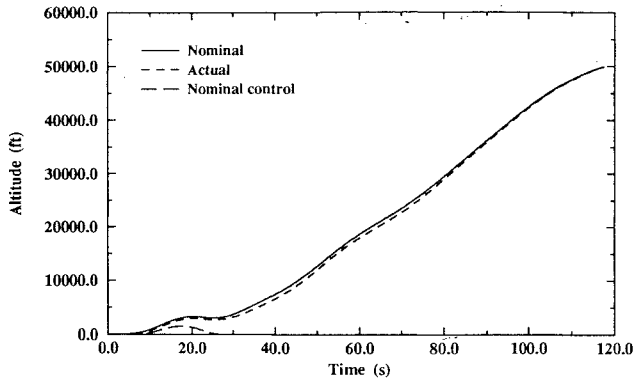


Fig. 5 Controller III: wind-disturbed altitude history.

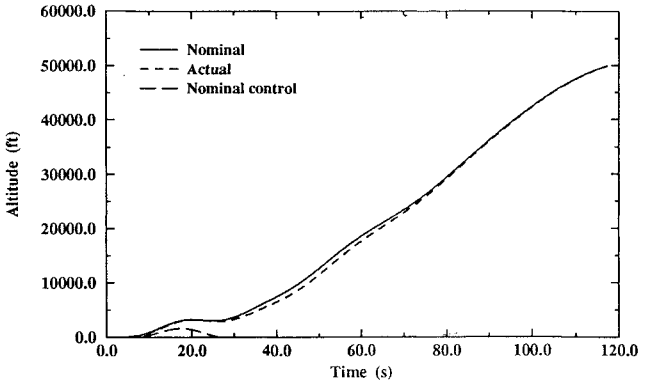


Fig. 6 Controller III: altitude history with −30% aerodynamic coefficient perturbation.

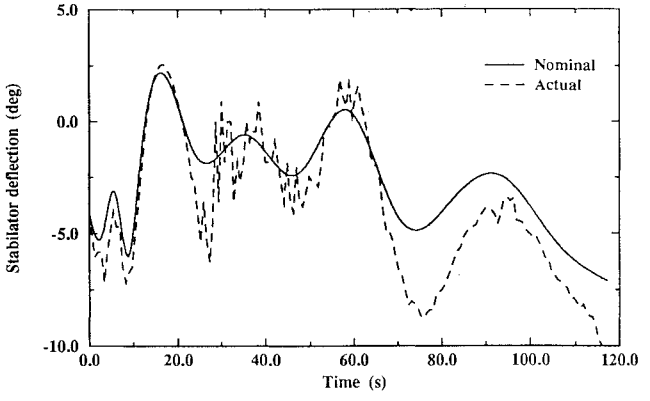


Fig. 7 Controller III: stabilator deflection history with −30% aerodynamic coefficient perturbation.

of system uncertainties. The nominal and actual stabilator deflection histories for the case of −30% errors are shown in Fig. 7. The actual stabilator deflection shows considerable modulation about the nominal to account for the modeling uncertainties. It should be mentioned that a 24 deg/s rate limit on the stabilator for the original model[8] was not enforced because it was felt that it was too restrictive and actuators with much higher rate limits are currently available.

## VI. Point-to-Point Control of Aircraft

In the preceding sections the aircraft is controlled to follow a precalculated trajectory. In some situations such as transition from one point to another, the desired trajectory may be chosen to have sufficiently simple form so that it can be designed onboard in real time. In this case the controllers developed above are particularly suitable for control purposes.

To explore this idea, assume that the current flight condition is specified by the values of the variables $y_i$, denoted by $y_{i0}$, $i = 1, \ldots, k$. The $y_i$ can be state variables or functions of state variables. The desired flight condition is defined by $y_{if}$. A simple design of the transition trajectory from the current condition to the desired

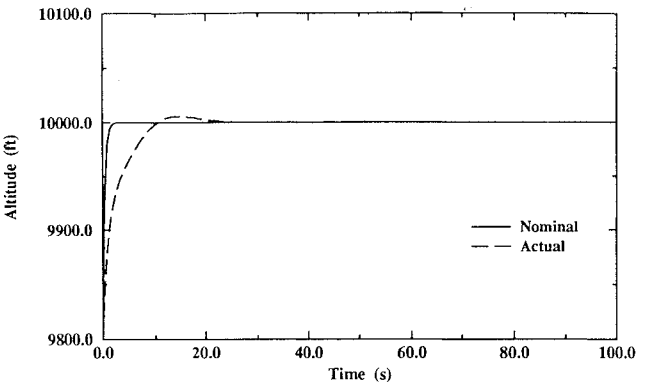


Fig. 8 Altitude history for task 1 (at 10,000 ft).

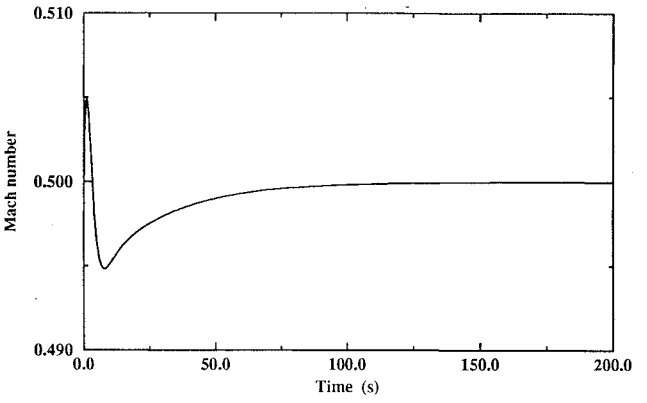


Fig. 9 Mach history for task 1 (at 10,000 ft).

condition can be

$$y_i^*(t) = (y_{i0} - y_{if})e^{-(t-t_0)/\tau_i} + y_{if}, \qquad i = 1, \ldots, k \quad (37)$$

where $\tau_i$ is a preselected time constant. Then $y_i^*(t)$ is treated as the reference history for $y_i(t)$ [denoted previously by $s(t)$ in Sec. II]. The controls needed to fly this trajectory are not explicitly defined. But we notice that the architecture of the controllers is such that no knowledge of the nominal controls is required. Hence, these controllers can be conveniently employed to control the aircraft to follow the trajectory defined by Eqs. (37).

We demonstrate this application by considering the AIAA 1991–1992 Controls Design Challenge.[8] The Design Challenge specifies several trajectories for testing candidate control designs as well as error bounds on critical flight parameters. Some of the maneuver tasks specified by the Design Challenge are:

1. Beginning at 9800 ft and Mach 0.5, climb 200 ft and hold altitude and Mach number, simultaneously.

2. Beginning at 39,800 ft and Mach 1.4, climb 200 ft and hold altitude and Mach number, simultaneously.

3. Accelerate from Mach 0.5 to Mach 1.4 while holding altitude at 30,000 ft.

The Challenge requires following these trajectories within an altitude error of ±50 ft and a Mach number error of within ±0.01. For brevity we restrict the flight in a vertical plane. The two controls available are the symmetric stabilator deflection and throttle setting. For the tasks addressed, the altitude and velocity must be controlled. To maintain an appropriate attitude of the aircraft, the pitch angle should also be controlled. Note that for the reasons mentioned in Sec. III (discontinuities caused by interpolation tables) and the fact that no reference controls are readily available, the standard linearization techniques are not applicable. Following the above-proposed approach, we identify $y_1 = h$, $y_2 = V$, and $y_3 = \theta$. For tasks 1 and 2, the initial and final altitudes are defined by the problem statement. The altitude reference history $h^*(t)$ is described by Eq. (37) with $\tau_h = 1.5$ s and $V^*(t) = \text{const}$. For task 3, the altitude reference history is a constant and $V^*(t)$ has the form of Eq. (37), with $\tau_V = 20$ s. For all cases, the initial pitch angle is 5 deg, the final pitch angle is the trim value for the specified altitude and Mach number, and

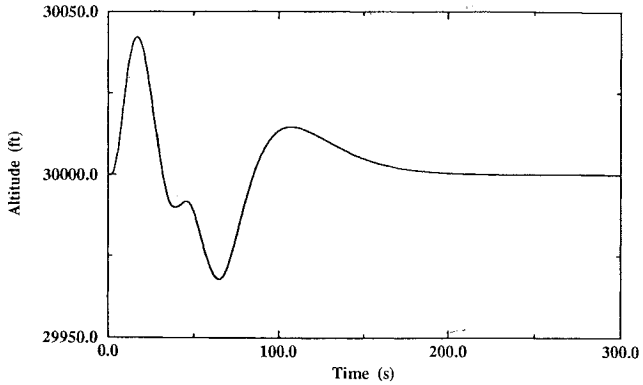


**Fig. 10 Altitude history for task 3.**

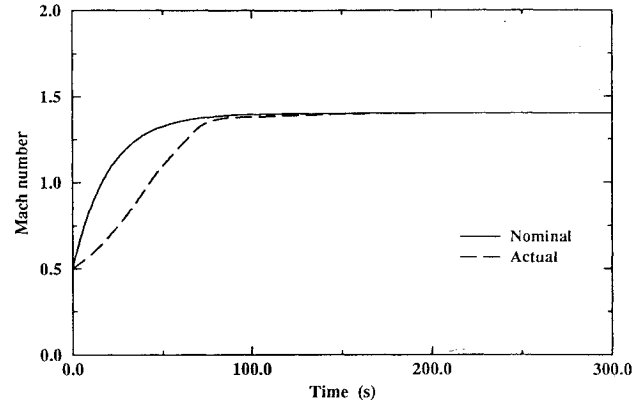


**Fig. 11 Mach history for task 3.**

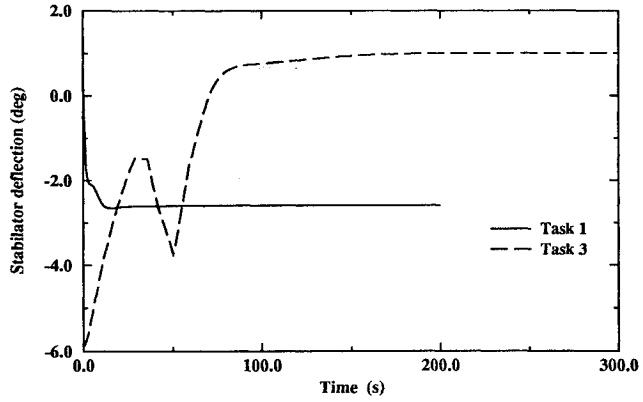


**Fig. 12 Stabilator deflection history for tasks 1 and 3.**

$\tau_\theta = 20$ s. Controller III with $\Delta = 1.0$ was employed to solve the three flight control problems successfully. All errors are well within the limits. Figures 8–11 show the altitude and Mach number histories for tasks 1 and 3. The reference altitude history for task 1 and reference Mach history for task 3 are also plotted in Figs. 8 and 11, respectively, for comparison. The stabilator deflection histories for the two cases are depicted in Fig. 12.

The calculation of Eq. (37) can be easily carried out onboard. In more general scenarios of point-to-point transition, the $y_{i0}$ can be assigned the current values of the variables of interest. The desired final values $y_{if}$ may be determined based on the current condition and mission objective. The controllers then can be used to guide the aircraft to make the required transition. An obvious application is to control an aircraft for precision landing in which simple analytical expressions similar to Eqs. (37) represent the glide slope and flare path. This technique may be incorporated into a head-up display to aid the pilot in landing, instructing him or her what the required controls should be. This could minimize the pilot stress in the landing of a carrier aircraft.

## VII. Conclusions

A newly developed methodology for design of nonlinear feedback controllers is applied to aircraft control. The approach is systematic, is easy to apply, and requires no stringent conditions on the system. Using a high-performance aircraft model, we show that the controller exhibits good performance under a variety of strenuous conditions. The performance of the baseline controller is further enhanced by continuously adjusting a controller parameter in an optimal fashion and including derivative feedback in the controller. In the presence of appreciable aerodynamic uncertainties and wind disturbance, the controller demonstrates strong robustness in that satisfactory performance is maintained. Finally, some of the tasks in the AIAA Controls Design Challenge are accomplished to illustrate the application of the controller in point-to-point control of aircraft.

## References

[1]Snell, S. A., Enns, D. F., and Garrard, W. L., "Nonlinear Inversion Flight Control for a Supermaneuverable Aircraft," *Journal of Guidance, Control, and Dynamics*, Vol. 15, No. 4, 1992, pp. 976–984.

[2]Lane, S. H., and Stengel, R. F., "Flight Control Design Using Nonlinear Inverse Dynamics," *Automatica*, Vol. 24, No. 4, 1988, pp. 471–483.

[3]Meyer, G., Su, R., and Hunt, L. R., "Application of Nonlinear Transformation to Automatic Flight Control," *Automatica*, Vol. 20, No. 1, 1984, pp. 103–107.

[4]Menon, P. K. A., Badgett, M. E., Walker, R. A., and Duke, E. L., "Nonlinear Flight Test Trajectory Controls for Aircraft," *Journal of Guidance, Control, and Dynamics*, Vol. 10, No. 1, 1987, pp. 62–77.

[5]Wise, K. A., "Nonlinear Aircraft Flight Control Using Dynamic Inversion," *Proceedings of American Control Conference*, Chicago, IL, June 1992.

[6]Franklin, J. A., Hynes, C. S., Hardy, G. H., Martin, J. L., and Innis, R. C., "Flight Evaluation of Augmented Controls for Approach and Landing of Powered-Lift Aircraft," *Journal of Guidance, Control, and Dynamics*, Vol. 9, No. 5, 1986, pp. 555–565.

[7]Lu, P., "Nonlinear Predictive Controllers for Continuous Systems," *Journal of Guidance, Control, and Dynamics*, Vol. 17, No. 3, 1994, pp. 553–560.

[8]Brumbaugh, R. W., "An Aircraft Model for the AIAA Controls Design Challenge," AIAA Paper 91-2631, Aug. 1991.

[9]Khan, M. A., "New Techniques in Trajectory Optimization and Guidance," M.S. Thesis, Iowa State Univ., Ames, IA, 1992.

[10]Lu, P., and Khan, M. A., "Nonsmooth Trajectory Optimization: An Approach Using Continuous Simulated Annealing," *Journal of Guidance, Control, and Dynamics*, Vol. 17, No. 4, 1994, pp. 685–691.

[11]Kahaner, D., Moler, C., and Nash, S., *Numerical Methods and Software*, Prentice-Hall, Englewood Cliffs, NJ, 1989, pp. 361–363.

[12]Zhao, Y., and Bryson, A. E., "Approach Guidance in a Downburst," *Journal of Guidance, Control, and Dynamics*, Vol. 15, 1992, pp. 893–900.